Sensors & Transducers, Vol. 182, Issue 11, November 2014, pp. 180-186

www.sensorsportal.com

Sensors & Transducers

http://www.sensorsportal.com

Math Model and Calculation Analysis of Inter-harmonic of Double PWM Speed Control System in Distribution Network

[1] Yang Wen-Huan, [1,*] Li Lu-Yang, [1] Li Zheng, [2] Li Rong-Gao

[1] School of Optical-Electrical and Computer Engineering, University of Shanghai for Science and Technology, Shanghai, 200093, China

[2] Tongsheng Electricity Power Company Ltd., Pudong District, Shanghai, 200122, China

[*] Tel.: 18818251193

[*] E-mail: liluyangnj@163.com

Received: 14 August 2014 /Accepted: 30 October 2014 /Published: 30 November 2014

Abstract: Aiming at the problem that the distribution network voltage will fluctuate because of the inter-harmonic currents injected into the network by double PWM speed control system when regulating the speed of the asynchronous motor, we established the inter-harmonic current math model of double PWM speed control system according to switching function based on a real bridge crane. The distribution law of the inter-harmonic is got by calculating the grid-side currents and their spectrum while letting the motor run at different quadrants and frequencies. The result which is verified by simulation and experiment shows that the content of the inter harmonic currents is more than that of harmonic currents in double PWM speed control system, the frequency of the inter harmonics of the grid-side current mainly focus on the scope lower than the fundamental frequency, and when the motor runs at low frequencies, the THD of the grid-side current is high. The result has verified the reason why the voltage of a bridge crane distribution system of a deepwater port in Shanghai flickers.

Keywords: Double PWM, Switching function, Grid-side current, Harmonics, Inter-harmonics.

1. Introduction

With the development of power electronic technology, double PWM converters are widely used in high power applications, which have low grid-side harmonics [1, 2]. But, as a result of the load fluctuation and the speed governing of asynchronous motor, the grid-side current contains inter-harmonics. When the number of double PWM converter reaches a certain amount, the voltage of the distribution network will flicker with inter-harmonic current frequency, which have has serious impact on the power quality in distribution networks and equipment connected into the network [3-5]. It is reported that the distribution network of a deepwater port in Shanghai has experienced low-frequency voltage flicker when too many bridge crane were put to use.

In recent years, scholars of different countries have carried out extensive research on the characteristics [6-8] and calculation methods [9-13] of inter-harmonics because of its great harm, and the results are applied to the analysis of HVDC transmission system and high power variable frequency speed regulation system [14-19]. Literature [18] establishes the mathematic model of AC speed control system based on switch function, but it doesn't analyze the inter-harmonic current of the system injected into the distribution network.

Literature [19] analyzed grid side inter-harmonic current of frequency converting speed regulating system with diode rectifier circuit. But diode rectifier can't pass energy to power grid, so the conclusion can't be used to analysis double PWM double PWM speed control system. So far, no report on research findings about grid side inter-harmonic current of double PWM speed control system can found.

In this paper, we establish inter-harmonic mathematical model of double PWM speed control system based on switch function. Then we calculate and analyze the harmonics and inter-harmonics injected into the power grid when asynchronous machine work at different frequencies by taking bridge crane used in the Port of Shanghai as a physical model. At last, some experiments are conducted. The results of the calculation and experiments show that the grid side current of double PWM speed control system has a certain amount of harmonics and inter-harmonics; inter-harmonics frequencies are mainly concentrated in the range below the net side current fundamental frequency; the amount of grid side inter-harmonic current will increase when the motor operates at a low frequency, so the THD of the grid side current is high. These results may explain why the voltage of power distribution system of bridge crane located in the deep-water port in Shanghai flicker.

Nomenclature

$-$	$\bar{x}$ is the DC components of x
$\sim$	$\tilde{x}$ is the AC components of x
x_N	x_N is the rated value of x
e_a	Voltage of power grid (also: e_b, e_c)
i_a	Grid side current of double PWM speed control system (also: i_b, i_c)
i_{A0},	Stator current of the motor (also: i_{B0}, i_{C0},)
i_c	Current of capacitor
i_{ca}	DC side current of motor side converter
i_{dc}	DC side current of grid side converter
$\dot{I}_1$	Stator current of the motor
$\dot{I}_2$	Rotor current of the motor
$\dot{I}_m$	Excitation current of the motor
L	Grid side equivalent inductance
m	Harmonic order of carrier
M	Modulation ratio
n	Harmonic order of Modulation wave
R	Sum of switching loss equivalent resistance and the equivalent resistance of transformer
R_1	Stator resistor
R_2	Rotor resistor converted to stator side
s	Slip
T_{em}	Load torque
S_k	Switch of grid side converter (k=a, b, c)
S_k'	Switch of motor side converter (k=a ,b, c)
s_k	Switch function of grid side converter (k=a, b, c)
s_{KO}	Switch function of grid side converter (k=a, b, c)
u_{dc}	DC link voltage
ω_l	Angular frequency of Modulation wave
ω_c	Angular frequency of carrier
Ω_1	Angular frequency of the motor
ϕ_Z	Equivalent impedance angle of the motor

2. Inter-harmonic Mathematic Model of Double PWM Speed Control System

The circuit of double PWM speed control system is shown in Fig. 1. As the figure shows, the system is consists of the equivalent models of power grid, two converters and a motor. Relevant variables and the reference direction are shown in this figure, too.

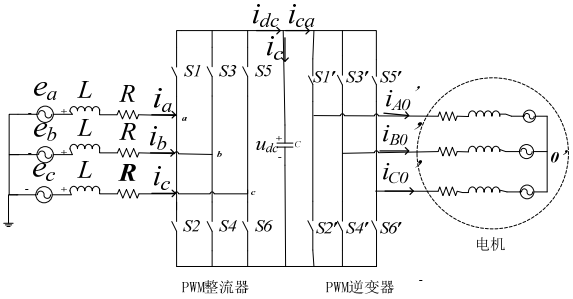

Fig. 1. Schematic of double PWM speed control system.

2.1. Mathematic Model of Grid Side PWM Converter

When writing the equation according to Kirchhoff's voltage law, the grid side current has the form (take i_a as example) [20]:

$$i_a = \frac{1}{L}\int e_a - \frac{1}{3}u_{dc}\left(2s_a - s_b - s_c\right)dt\,, \qquad (1)$$

When using the symmetrical switch sampling, the expression can be expanded into the following form by using Fourier series:

$$s_a = 0.5 + 0.5M\sin(\omega t - \theta) + \sum_{n=1}^{\infty}(-1)^n \frac{2}{n\pi}\sin\pi n[0.5\cos(n\omega_s t) + 0.5M\sin(\omega t - \theta)\cos(n\omega_s t)], \qquad (2)$$

u_{dc} can be expanded into the sum of its DC component and AC component, so the switching function expression of grid side current is:

$$i_a = \frac{1}{L}\int e_a dt - \frac{\bar{u}_{dc}}{3L}\int [2s_a - (s_b + s_c)]dt - \frac{1}{3L}\int [2s_a - (s_b + s_c)]\tilde{u}_{dc} dt \quad , \quad (3)$$

Eq. (3) shows that grid side harmonic current and AC component of u_{dc} have great relationship.

Similarly, i_b, i_c can be described.

The relationship between i_{dc} and i_a, i_b, i_c is:

$$i_{dc} = i_a s_a + i_b s_b + i_c s_c , \quad (4)$$

2.2. Mathematic Model of DC Bus Voltage Fluctuation

By using Kirchhoff's current law at the positive node of the capacitor, u_{dc} has the form [21, 22]:

$$C\frac{du_{dc}}{dt} = i_{dc} - i_{ca} , \quad (5)$$

Eq.(5) shows that the fluctuation component of u_{dc} can be caused by the fluctuation of e_a, e_b, e_c, the change of i_{ca}, and the motor speed regulating:

$$\begin{aligned} u_{dc} &= \tilde{u}_{dc} + \bar{u}_{dc} \\ i_{dc} &= \tilde{i}_{dc} + \bar{i}_{dc} \\ i_{ca} &= \tilde{i}_{ca} + \bar{i}_{ca} \end{aligned} , \quad (6)$$

It's not hard to get expression of DC link by substituting Eq.(6) in Eq.(5):

$$\begin{aligned} C\frac{du_{dc}}{dt} &= C\left(\frac{d\tilde{u}_{dc}}{dt} + \frac{d\bar{u}_{dc}}{dt}\right) \\ &= (\tilde{i}_{dc} + \tilde{i}_{dc}) - (\tilde{i}_{ca} + \tilde{i}_{ca}) \end{aligned} , \quad (7)$$

The AC expression is:

$$\tilde{i}_{dc} = C\frac{d\tilde{u}_{dc}}{dt} + \tilde{i}_{ca} , \quad (8)$$

The DC expression is:

$$\bar{i}_{dc} = C\frac{d\bar{u}_{dc}}{dt} + \bar{i}_{ca} = \bar{i}_{ca}$$

So:

$$\bar{i}_{dc} = \bar{i}_{ca} , \quad (9)$$

It's not hard to find that the DC component can be transmitted between grid side and motor side. The AC component can be expressed as:

$$\begin{aligned} \tilde{i}_{ca} &= \sum_{\nu=1}^{\infty} I_{cn}\cos(\nu\omega_{ca}t) \\ \tilde{i}_{dc} &= \sum_{\lambda=1}^{\infty} I_{d\mathrm{m}}\cos(\lambda\omega_d t) \end{aligned} , \quad (10)$$

In this expression, ω_d and ω_{ca} are the frequency of $\tilde{i}_{dc}$ and $\tilde{i}_{ca}$ respectively. $\nu\,(\nu > 0)$ is the harmonic order of ω_{ca}; $\lambda\,(\lambda > 0)$ is the harmonic order of ω_{d}. The capacitive current is:

$$C\frac{d\tilde{u}_{dc}}{dt} = \sum_{\lambda=1}^{\infty} I_{d\lambda\mathrm{m}}\cos(\lambda\omega_d t) - \sum_{\nu=1}^{\infty} I_{c\nu n}\cos(\nu\omega_{ca}t) , \quad (11)$$

$$\begin{aligned} \tilde{u}_{dc} &= \frac{1}{C}\int\left[\sum_{\lambda=1}^{\infty} I_{d\lambda}\cos(\lambda\omega_d t) - \sum_{\nu=1}^{\infty} I_{c\nu}\cos(\nu\omega_{ca}t)\right]dt \\ &= \sum_{\lambda=1}^{\infty}\frac{I_{d\lambda}}{\lambda\omega_d C}\sin(\lambda\omega_d t + \beta) - \\ &\quad \sum_{\nu=1}^{\infty}\frac{I_{c\nu}}{\nu\omega_{ca}C}\sin(\omega_{ca}t + \gamma) \end{aligned} , \quad (12)$$

Eq. (12) shows that the lower the frequency is, the greater the voltage will fluctuates. Eq.(3) shows that the bigger the AC component of u_{dc} is, the more inter-harmonic grid side current will have, especially low frequency inter-harmonic current.

We set:

$$\frac{I_{c\lambda}}{\lambda\omega_d C} = \frac{I_{d\nu}}{\nu\omega_{ca}C} = \frac{I_m}{\omega_0 C} , \text{ and } \omega_d \neq \omega_{ca} ,$$

then:

$$\tilde{u}_{dc0} = \frac{2I_{\mathrm{m}}}{\omega_0 C}\left[\cos\frac{(\omega_d + \omega_{ca})t + (\beta + \gamma)}{2} * \sin\frac{(\omega_d - \omega_{ca})t + (\beta - \gamma)}{2}\right] , \quad (13)$$

Eq.(13) shows that the capacitor has significant effect to inhibit the AC component of i_{dc} and i_{ca}, the bigger the capacitance is, the less the AC component pass through the DC link is. For the grid side converter: the fundamental frequency is always 50 Hz, so the frequency of the fluctuation injected into DC link is relatively high and fixed; the filtering effect of the capacitor is obvious.

Because of the speed regulating especially low frequency starting, the motor side converter often works in several Hz. Therefore, the filtering effect of the capacitor is limited, and low frequency fluctuation has strong ability to pass through the capacitor and inject into the grid. So, it is easy for the motor's low frequency signal to inject into the power grid.

2.3. Mathematic Model of Motor and Motor Side PWM Converter

The switching function can be described as follows when the converter use synchronous SPWM modulation and the starting point of sine wave is the zero crossing of the fall edge of the triangular carrier [21-24]:

$$s_{AO'} = \frac{M}{2}\sin(\omega_l t) + \frac{2}{\pi}\sum_{m=1,3,5\cdots}^{\infty}\frac{J_0(mM\frac{\pi}{2})}{m}\cdot\sin\left[mN(\omega_l t)\right] + \frac{2}{\pi}\sum_{m=1,3,5\cdots}^{\infty}\sum_{n=\pm2,\pm4\cdots}^{\pm\infty}\frac{J_n(mM\frac{\pi}{2})}{m}\sin\left[(mN+n)(\omega_l t)\right] + \frac{2}{\pi}\sum_{m=2,4\cdots}^{\infty}\sum_{n=\pm1,\pm3,\pm5\cdots}^{\pm\infty}\frac{J_n(mM\frac{\pi}{2})}{m}\sin\left[(mN+n)(\omega_l t)\right] \quad (14)$$

where J_0 and J_n are zero order Bessel function of the first kind, 0 and n are the order of them respectively.

$$J_n(z) = \frac{1}{2\pi}\int_{-\pi}^{\pi}\cos(n\theta - z\sin\theta)d\theta, \quad (15)$$

According to the principle of electro mechanics, there is constraint relationship of three phase squirrel cage asynchronous motor:

$$T_{em} = \frac{1}{\Omega_1}3I_2^2\frac{R_2}{s}, \quad (16)$$

According to T type equivalent circuit of motor, the stator current $\dot{I}_1$ can be described as:

$$\dot{I}_1 = \dot{I}_2^{'} + \dot{I}_m, \quad (17)$$

If $\dot{I}_m$ is ignored, i_A can be described as:

$$i_A = \sqrt{2}I_1\cos\left(\omega t - \phi_Z\right), \quad (18)$$

According to the way the motor side converter works, $i_{AO'}$ can be describe as:

$$i_{AO'} = s_{AO'}i_A, \quad (19)$$

Similarly, $i_{BO'}, i_{CO'}$ can be described.

The relationship between i_{ca} and $i_{AO'}$ $i_{BO'}$ $i_{CO'}$ can be described as:

$$i_{ca} = i_{AO'}s_{AO'} + i_{BO'}s_{BO'} + i_{CO'}s_{CO'}, \quad (20)$$

The inter-harmonic mathematic model of double PWM speed control system is constituted by Eq.(1), (2), (3), (4), (5), (14)~(20).

3. Calculation and Analysis of Inter-harmonics

3.1. Calculation Process of Inter-harmonics

According to the mathematic model of the derived in last section, the grid side currents of the double PWM speed control system under different working conditions can be calculated. The calculation flow is shown in Fig. 2.

According to the flow shown in Fig. 2, this paper chooses a three phase squirrel cage asynchronous motor used in the bridge crane. Its parameters are shown as follows: e_{aN}, e_{bN}, e_{cN} are 400 V, rated frequency is 50 Hz, T_{emN} is 5760 N·m, R1 is 7 mΩ, R2 is 1.98 mΩ, stator leakage reactance is 0.655 Ω, rotor leakage reactance is 0.0276 Ω, sN is 0.0067, pole pairs are 2.

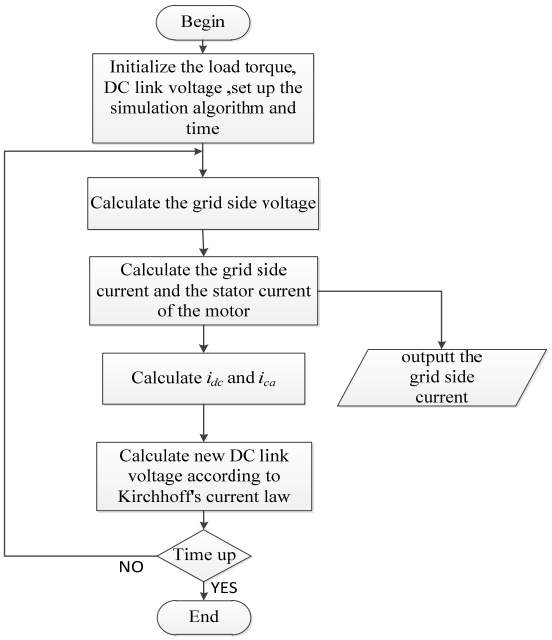

Fig. 2. The calculation flow chart.

3.2. Calculation and Analysis

In this paper, the motor is set to drag the potential energy load, and work at the state of motor and generator respectively. The frequencies of the motor's stator voltage range from 5 Hz to 50 Hz, and take 10 Hz as the step value. The results are as Fig. 3 and Fig. 4.

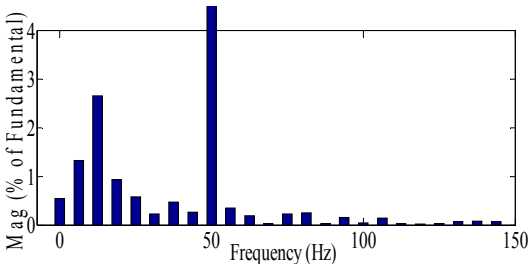

(a) the spectrum of grid side current when the motor works at 15 Hz.

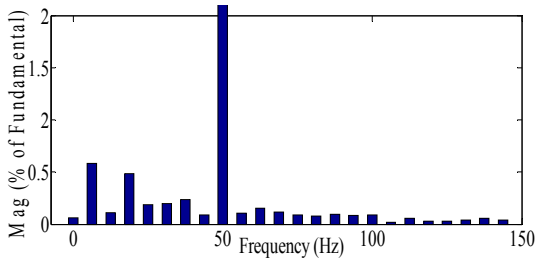

(b) the spectrum of grid side current when the motor works at 45 Hz.

Fig. 3. The spectrum of grid-side current when lifting the weight.

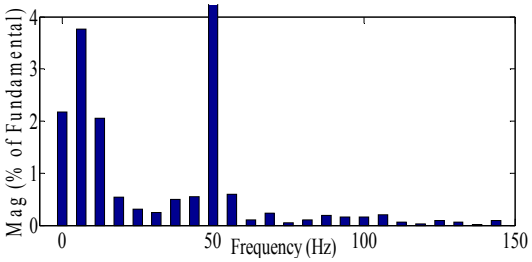

(a) the spectrum of grid side current when the motor works at 15 Hz.

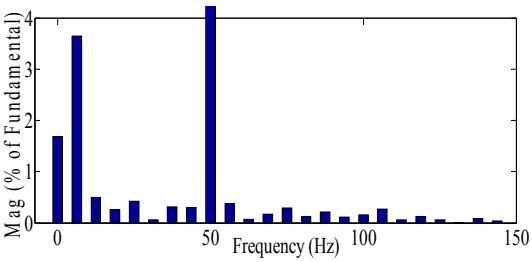

(b) the spectrum of grid side current when the motor works at 45 Hz.

Fig. 4. The spectrum of grid-side current when dropping the weight.

As shown in Fig. 3 and Fig. 4, the gird side current include not only harmonics but also inter-harmonics. The inter-harmonic frequencies mainly concentrate in the range below the fundamental frequency of grid side voltage. Besides, the calculation results show that when the motor works in the condition of generator, the inter-harmonic injected into the network by grid side PWM converter is higher than that when it works at the motor state.

Furthermore, along with the increase of the operating frequency of the motor side converter, harmonic current and inter-harmonic current decreased. The change relationship between grid side current THD value and the operating frequency of the motor side converter is shown in Fig. 5.

Fig. 5 shows that when motor side converter operates in rated frequency, THD value of grid side current is the lowest. But the filtering effect of the capacitor is limited when the motor start at low frequency.

Therefore, it is easier for low frequency fluctuation to transmit to the power grid, and the THD value of grid side current is the largest.

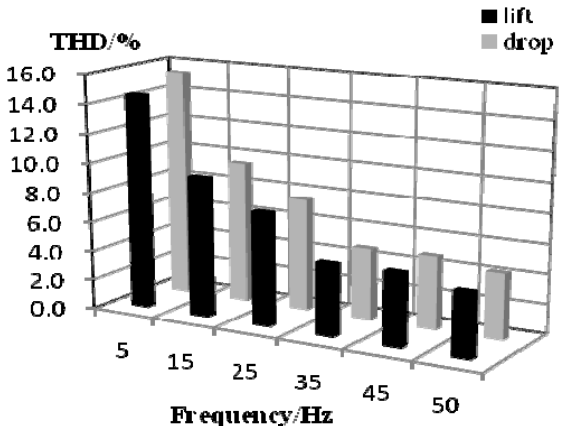

Fig. 5. THD of grid-side current in different condition.

4. Experiment Analysis

In order to verify the validity of the calculation method, relevant experiments have been done in a real bridge crane.

As shown in Fig. 6 and Fig. 7, grid side power factor is high, and the waveform of current is sinusoids, but the amplitude changes. It proves the existences of inter-harmonic of grid side current.

The spectrum shows that the content of grid side inter-harmonic when the motor works at 45 Hz is significantly less than that when it works at 15 Hz. But the common features of both are: the frequencies of inter-harmonic mainly concentrate in the range below the fundamental frequency of grid side voltage. It is consistent with the simulation results, so the effectiveness of the calculation model and the correctness of the conclusion are verified.

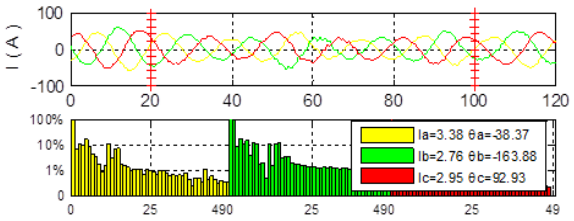

(a) the grid side current and its spectrum when the motor works at 15 Hz.

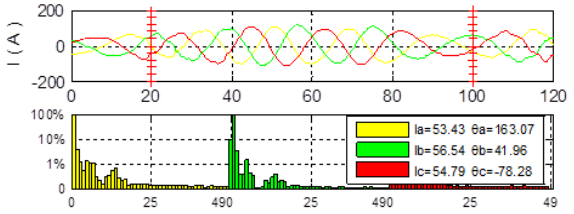

(b) the grid side current and its spectrum when the motor works at 45 Hz.

Fig. 6. The grid-side current and its spectrum when lifting the weight.

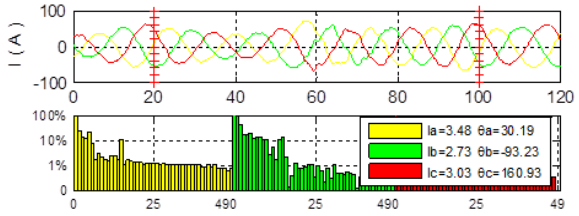

(a) the grid side current and its spectrum when the motor works at 15 Hz.

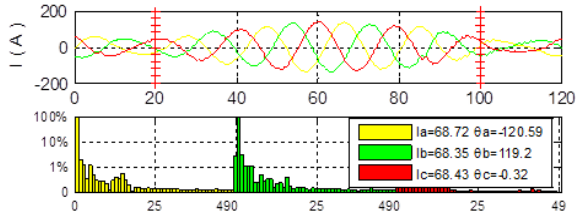

(b) the grid side current and its spectrum when the motor works at 45 Hz.

Fig. 7. The grid-side current and its spectrum when dropping the weight.

5. Conclusion

By calculating the grid side inter-harmonic current when the motor operates at different states and frequencies and comparing with the experimental results, this paper has got following conclusions:

1) The inter-harmonic content injected into the power grid by grid side PWM converter of double PWM converter is larger than the harmonic content.

2) Inter-harmonic frequency mainly concentrates in the range below the fundamental frequency of grid side voltage. The THD value of grid side current is larger when the motor operates at low frequency.

3) Grid side inter-harmonic current is larger when the motor operates at the state of generator than that when it operator at the state of motor. THD has little difference.

This paper has designed the calculation flow of the grid side inter-harmonic current of double PWM speed control system based on its mathematic model; revealed the distribution law of spectrum of grid side inter-harmonic current; and proved the effectiveness of the calculation model and the correctness of the conclusions. The model and conclusions have practical significance for inhibiting the voltage flicker caused by inter-harmonic in distribution network.

Acknowledgments

This article and relevant project is supported by following two foundations: 1) Shanghai Science and Technology Committee (11DZ1201802); 2) The Hujiang Foundation of China (B1402/D1402).

References

[1]. Wan-Wei Wang, Hua-Jie Yin, Guang Lin, Dual-PWM frequency-variable speed regulation system based on direct power control, *Journal of South China University of Technology (Natural Science Edition)*, Vol. 39, No. 3, 2011, pp. 67-72.

[2]. J. Li-Ping, Q. Xiao-Yan, Z. Rui-Wei, Development, present situation and application of dual PWM converter, *China Science and Technology Information*, Issue 10, 2008.

[3]. V. B. Virulkar, M. V. Aware, Modeling and simulation of flicker due to interharmonics, in *Proceedings of the IEEE India International Conference on Power Electronics (IICPE)*, 2011, pp. 1-5.

[4]. J. Wang, H. Liu, A calculation method for interharmonics-caused flicker and flicker source identification, *Automation of Electric Power Systems*, Vol. 35, Issue 12, 2011, pp. 52-58.

[5]. Xiong Jiefeng, Li Qun, Yuan Xiaodong, Chen Bing, Yang Zhichao, Wang Bolin, Detection methods of harmonics and interharmonics in power system, *Automation of Electric Power Systems*, Issue 11, 2013, pp. 125-133.

[6]. D. Zhang, W. Xu, Y. Liu, On the phase sequence characteristics of interharmonics, *IEEE Transactions on Power Delivery*, Vol. 20, Issue 4, 2005, pp. 2563-2569.

[7]. J. Yong, T. Tayjasanant, X. Wilsun, et al, Characterizing voltage fluctuations caused by a pair of interharmonics, *IEEE Transactions on Power Delivery*, Vol. 23, Issue 1, 2008, pp. 319-327.

[8]. T. Tayjasanant, W. Wang, C. Li, et al, Interharmonic-flicker curves, *IEEE Transactions on Power Delivery*, Vol. 20, Issue 2, 2005, pp. 1017-1024.

[9]. D. Sharmitha, Estimation of harmonics and interharmonics using phaselocked loop, in

Proceedings of the International Conference on Power, Energy and Control, 2013, pp. 514-519.
[10]. S. R. Hadian Amrei, D. Xu, Y. Lang, A new approach to harmonics and interharmonics generation in general VSI/CSI converters, in *Proceedings of the 37th IEEE Power Electronics Specialists Conference, (PESC'06)*, 2006, pp. 1-7.
[11]. M. Li, X. Wang, An autoregressive model algorithm for the inter-harmonic spectral estimation in the power system, *Proceedings of the CSEE*, Vol. 30, Issue 1, 2010, pp. 72-76.
[12]. Y. Liu, J. Hui, H. Yang, Multilayer DFT interpolation correction approach for power system harmonic analysis, *Proceedings of the Chinese Society of Electrical Engineering*, Vol. 32, Issue 25, 2012, pp. 182-188.
[13]. J. Wang, H. Liu, H. Xiao, An approach to measure interharmonics-flicker based on synchronous demodulation, *Proceedings of the CSEE*, Vol. 31 (Supplement), 2011, 67-72 (in Chinese).
[14]. B. Geethalakshmi, K. Babu, S. S. Santhoshma, Analysis of interharmonics in conventional and matrix converter fed adjustable speed drives, in *Proceedings of the IEEE 5th India International Conference on Power Electronics (IICPE)*, 2012, pp. 1-6.
[15]. Q. Li, H. Liu, Z. Li, et al, Analysis on interharmonics generation in the asynchronous interconnection HVDC system, *Southern Power System Technology*, Issue 2, 2008, pp. 49-53.
[16]. L. Hu, R. Yacamini, Calculation of harmonics and interharmonics in HVDC schemes with low DC side impedance, *IEE Proceedings Generation, Transmission and Distribution*, Vol. 140, Issue 6, 1993, pp. 469-476.
[17]. D. J. Hume, A. R. Wood, C. M. Osauskas, Frequency-domain modelling of interharmonics in HVDC systems, *IEE Proceedings-Generation, Transmission and Distribution,* Vol. 150, Issue 1, 2003, pp. 41-48.
[18]. R. Carbone, F. De Rosa, R. Langella, et al, A new approach for the computation of harmonics and interharmonics produced by line-commutated AC/DC/AC converters, *IEEE Transactions on Power Delivery*, Vol. 20, Issue 3, 2005, pp. 2227-2234.
[19]. D. Basic, Input current interharmonics of variable-speed drives due to motor current imbalance, *IEEE Transactions on Power Delivery*, Vol. 25, Issue 4, 2010, pp. 2797-2806.
[20]. Z. Chong-Wei, Z. Xing, PWM rectifier and its control, *China Machine Press*, Beijing, 2012, pp. 49-53 (in Chinese).
[21]. R. Carbone, D. Menniti, R. E. Morrison, et al, Harmonic and interharmonic distortion modeling in multiconverter systems, *IEEE Transactions on Power Delivery*, Vol. 10, Issue 3, 1995, pp. 1685-1692.
[22]. L. Xinjun, Z. Min, Harmonic analysis of three-phase SPWM inverter and its inhibition scheme, *Explosion-Proof Electric Machine,* Issue 1, 2008, pp. 18-20, 32.
[23]. Gary W. Chang, Shin-Kuan Chen, An analytical approach for characterizing harmonic and interharmonic currents generated by VSI-fed adjustable speed drives, *IEEE Transactions on Power Delivery*, Vol. 20, Issue 4, 2005, pp. 2585-2593.
[24]. Gary W. Chang, Shin-Kuan Chen, Huai-Jhe Su, et al, Accurate assessment of harmonic and interharmonic currents generated by VSI-fed drives under unbalanced supply voltages, *IEEE Transactions on Power Delivery*, Vol. 26, Issue 2, 2011, pp. 1083-1091.